Proceedings of the 2003 IEEE
International Conference on Robotics & Automation
Taipei, Taiwan, September 14-19, 2003

Running Pattern Generation and Its Evaluation Using a Realistic Humanoid Model

Takashi Nagasaki*1, Shuuji Kajita*2, Kazuhito Yokoi*2, Kenji Kaneko*2, Kazuo Tanie*1*2

*1 *University of Tsukuba,*
*2 *National Institute of Advanced Industrial Science and Technology(AIST)*
E-mail: t-nagasaki@aist.go.jp

Abstract

This paper describes a possibility of running humanoid robot based on the physical properties of an existing humanoid robot HRP-2L. To generate running motion, we develop a general method to control the total linear/angular momentum of multi-link system. By this method, we can generate a reliable running pattern. Conducting simulations which take into account of physical restrictions, we show that our humanoid robot can run at least with 0.5[m/s].

1 Introduction

Research on humanoid robots is currently one of the most exciting topics in the field of robotics and there exist many ongoing projects [2][4][6][11][16]. Most of them are focusing on biped walking as an important subject and have already demonstrated reliable dynamic biped walking. Watching those successful demonstrations, one can ask a natural question, "Can we build a running humanoid?"

We believe it is worthwhile as a technical challenge from the following reasons. First, study of running will add new functions of mobility to humanoid robots. For example, jumping over large obstacles or a fissure might be realized by a derivative of the running control. Second, studying extreme situation will give us an insight to improve the hardware itself. Current robots are too fragile to operate in the various environments. Even in an experiment of walking at low speed, we must treat them carefully. We are expecting to overcome this fragility in the process of developing a running humanoid.

Running robots have intensively studied by Raibert and his colleague [13]. Their famous hopping robots driven by pneumatic and hydraulic actuators performed various actions including somersault [12]. Using similar control strategy, Hodgins simulated running human in the computer graphics [5].

Ahmadi and Buehler studied running monopods from a standpoint of energy efficiency. Their ARL Momopod II[1] is an electrically powered running robot of 18[kg] weight and could run at 1.25[m/s] with a power expenditure of only 48[W].

All of those robots have spring mechanism to retrieve the kinetic energy in running cycles. It is obvious that such spring helps running but they might prevent the ordinal humanoid activities like walking, carrying an object, etc. Since our intention is to add a running function to a versatile humanoid robot, we start with a mechanism without springs. A similar approach is taken by Gienger et al.[2].

In our previous report, we investigated a running motion of an existing humanoid robot HRP-1 of 1.6[m] height and 117[kg] weight, which was developed in the Humanoid Robotics Project (HRP) of the Ministry of Economy, Trade and Industry of Japan. To generate a running pattern we proposed a method based on a simple inverted pendulum with some ad hoc modifications to absorb the modeling error. From our simulation, it turned out that we require unrealizable power of over 7[kW] for some actuators of HRP-1 running at 2.9[m/s].

In this paper, we examine a lighter biped robot HRP-2L which was also developed in HRP. For running pattern generation, we introduce a new method using precise physical parameters of a robot. After discussing a hopping pattern for less power consumption, we show a realistic running under the consideration of the actuator limits.

2 Humanoid Model

To build a running humanoid with conventional actuators, we must make it as light as possible. However, there is a physical and technical limitation for weight saving. Therefore we decided to set the model parameter based on the specification of an existing humanoid robot.

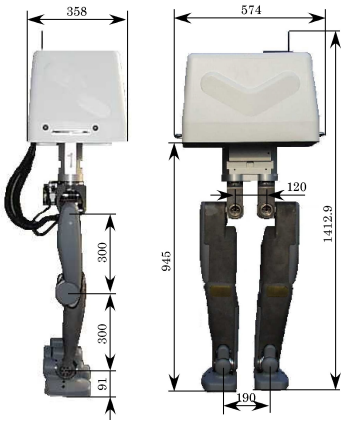

Figure 1: *HRP-2L*

2.1 HRP-2L

HRP-2L(Figure 1) is a biped robot that was developed in the Humanoid Robotics Project(HRP) of the Ministry of Economy, Trade and Industry of Japan[10]. Table 1 shows the specification of HRP-2L, and Table 2 shows the specification of leg actuators. HRP-2L has batteries and dummy weights, and these elements can be easily removed. Removing them and considering the little increase of weight for optional equipment for running, we assume that weight of HRP-2L will be reduced to 30[kg]. This is about one-fourth of the HRP-1 weight:117[kg].

HRP-2L has rubber bushs at each foot part. These compliance elements are effective in reducing the landing impact force and torque.

2.2 Actuator limits

Following two points should be taken into consideration as a limit of the motor capability.

The first point is maximum torque and speed. Generally, there is a relationship about a motor as follows,

$$\tau = K_T i \tag{1}$$

$$V = K_E \omega + R_a i \tag{2}$$

where τ is motor torque, i is motor current, V is motor voltage, ω is angular velocity, K_T and K_E are torque constant and back electro-motive force constant, R_a is armature resistance. The maximum torque is determined by the maximum current i_{max} which can be supplied to a motor and the maximum speed is mainly related with maximum voltage V_{max} which can be applied. i_{max} is restricted by the capability of a motor driver, and V_{max} is determined by the power supply voltage. From the specification

Table 1: *Specification of HRP-2L*

Size	6D.O.F/Legs(Hip:3 Knee:1 Ankle:2)	
	Upper leg length:	300[mm]
	Lower leg length:	300[mm]
	Ankle length:	91[mm]
	Length between hip joints:	120[mm]
Weight	Legs:8.6[kg/leg]×2[legs] =	17.2[kg]
	Batteries:	11.4[kg]
	Controller:	7.0[kg]
	Dummy Weights:	22.6[kg]
	Total:	58.2[kg]

Table 2: *Actuator specification of HRP-2L*

Joint		Actuator
Hip	Yaw	20[W]
	Roll	90[W]
	Pitch	90[W]
Knee	Pitch	150[W]
Ankle	Pitch	90[W]
	Roll	70[W]

of motor drivers of HRP-2L, i_{max} is 20$[A]$, V_{max} is 48$[V]$. To represent actuator limits in the simulation, the calculated motor current is saturated by i_{max}. For maximum voltage, instead of simulating the power supply in detail, we check whether the calculated motor voltage is lower than V_{max}. If the calculated motor voltage does not exceed the limit, it implies that the running motion is possible under the given power supply.

The second point is the restriction about the heat generation of a motor. If heat generation of a motor is large, a rotor can burn out. For this reason, the temperature of a rotor must not exceed the permitted value. We can calculate the temperature of a rotor as follows,

$$\delta_R = \delta_U + P_J R_{th}(1 - e^{\frac{-t}{\tau_{th}}}) \tag{3}$$

$$R_{th} = R_{th1} + R_{th2} \tag{4}$$

where t is time, δ_R is rotor temperature, δ_U is ambient temperature,P_J is heat generation of a motor, R_{th1}/R_{th2} is thermal resistance rotor-housing/housing-ambient and τ_{th} is thermal time constant. If the temperature of a rotor reaches permitted temperature too quick, a robot can not perform the running motion. As the guideline of the duration, we specify 30[s] or more operation time under the permitted temperature.

3 Momentum equation

To derive our new method of running pattern generation, this section shows the basic relationship between robot motion and its linear/angular momentum.

3.1 Momentum and joint velocities

We represent a humanoid robot as a mechanism of tree structure whose root is the base link (pelvis), a free-flying rigid body having 6 D.O.F in Cartesian space (Figure 2). We define the frame Σ_B at the center of the base link whose translational velocity and angular velocity are $\boldsymbol{v}_B(3\times 1)$ and $\boldsymbol{\omega}_B(3\times 1)$, respectively. In addition, we define the column vector $\dot{\boldsymbol{\theta}}(n\times 1)$ which contains velocities of all joints as its elements, where n is the number of joints. The linear momentum $\boldsymbol{P}(3\times 1)$ and the angular momentum $\boldsymbol{L}(3\times 1)$ of the whole mechanism are given by

$$\begin{bmatrix} \boldsymbol{P} \\ \boldsymbol{L} \end{bmatrix} = \begin{pmatrix} \tilde{m}\boldsymbol{E} & -\tilde{m}\widehat{\boldsymbol{r}_{B\to c}} & \boldsymbol{M}_{\dot{\theta}} \\ \boldsymbol{0} & \tilde{\boldsymbol{I}} & \boldsymbol{H}_{\dot{\theta}} \end{pmatrix} \begin{bmatrix} \boldsymbol{v}_B \\ \boldsymbol{\omega}_B \\ \dot{\boldsymbol{\theta}} \end{bmatrix}, \tag{5}$$

where $\tilde{m}$ is the total mass of the robot, $\boldsymbol{E}$ is an identity matrix of 3×3, $\boldsymbol{r}_{B\to c}(3\times 1)$ is the vector from the base link to the total center of mass (CoM), $\tilde{\boldsymbol{I}}(3\times 3)$ is the inertia matrix with respect to the CoM. $\boldsymbol{M}_{\dot{\theta}}(3\times n)$ and $\boldsymbol{H}_{\dot{\theta}}(3\times n)$ are the inertia matrices which indicate how the joint speeds affect to the linear momentum and the angular momentum respectively. $\widehat{\ }$ is an operator which translates a vector of 3×1 into a skew symmetric matrix 3×3 which is equivalent to a cross product.

In this paper, we represent the vector of position, velocity, angular velocity and related matrices are represented in Cartesian frame fixed on the ground.

3.2 Constraints of foot contact

Eq.(5) gives the total momentum of the robot in flight phase. However, when the robot is in contact with the ground, we must consider the constraints that reduce the total D.O.F of the system. The foot velocities $(\boldsymbol{v}_{F_i}, \boldsymbol{\omega}_{F_i})$ for the frame $\Sigma_{F_i}(i=1,2)$ are given by

$$\begin{bmatrix} \boldsymbol{v}_{F_i} \\ \boldsymbol{\omega}_{F_i} \end{bmatrix} = \begin{pmatrix} \boldsymbol{E} & \widehat{\boldsymbol{r}_{B\to F_i}} \\ \boldsymbol{0} & \boldsymbol{E} \end{pmatrix} \begin{bmatrix} \boldsymbol{v}_B \\ \boldsymbol{\omega}_B \end{bmatrix} + \boldsymbol{J}_{leg_i}\dot{\boldsymbol{\theta}}_{leg_i}, \tag{6}$$

where $\boldsymbol{J}_{leg_i}(6\times 6)$ is the Jacobian matrix calculated from the leg configuration, $\boldsymbol{r}_{B\to F_i}(3\times 1)$ is the position vector from the base link to the foot frame and $\dot{\boldsymbol{\theta}}_{leg_i}(6\times 1)$ is the joint speed vector of each leg. In this paper, we assume the number of joint of each leg is six. If $\boldsymbol{J}_{leg_i}$ is non singular, the velocities of the leg joint are given by

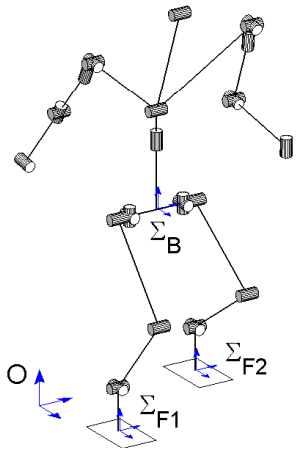

Figure 2: *A model of humanoid robot*

$$\dot{\boldsymbol{\theta}}_{leg_i} = \boldsymbol{J}_{leg_i}^{-1}\begin{bmatrix} \boldsymbol{v}_{F_i} \\ \boldsymbol{\omega}_{F_i} \end{bmatrix} - \boldsymbol{J}_{leg_i}^{-1}\begin{pmatrix} \boldsymbol{E} & \widehat{\boldsymbol{r}_{B\to F_i}} \\ \boldsymbol{0} & \boldsymbol{E} \end{pmatrix}\begin{bmatrix} \boldsymbol{v}_B \\ \boldsymbol{\omega}_B \end{bmatrix}. \tag{7}$$

Let us separate the joint speed vector into leg parts and the rest part as

$$\dot{\boldsymbol{\theta}} = [\dot{\boldsymbol{\theta}}_{leg_1}^T \quad \dot{\boldsymbol{\theta}}_{leg_2}^T \quad \dot{\boldsymbol{\theta}}_{free}^T]^T. \tag{8}$$

In Eq.(7), $\dot{\boldsymbol{\theta}}_{free}((n-12)\times 1)$ contains the joint speed for waist, arms and head. Then, we can rewrite the momentum equation as

$$\begin{bmatrix} \boldsymbol{P} \\ \boldsymbol{L} \end{bmatrix} = \begin{pmatrix} \tilde{m}\boldsymbol{E} & -\tilde{m}\widehat{\boldsymbol{r}_{B\to c}} \\ \boldsymbol{0} & \tilde{\boldsymbol{I}} \end{pmatrix}\begin{bmatrix} \boldsymbol{v}_B \\ \boldsymbol{\omega}_B \end{bmatrix} + \sum_{i=1}^{2}\begin{pmatrix} \boldsymbol{M}_{leg_i} \\ \boldsymbol{H}_{leg_i} \end{pmatrix}\dot{\boldsymbol{\theta}}_{leg_i} + \begin{pmatrix} \boldsymbol{M}_{free} \\ \boldsymbol{H}_{free} \end{pmatrix}\dot{\boldsymbol{\theta}}_{free}, \tag{9}$$

where

$$\begin{aligned} [\boldsymbol{M}_{leg_1}\boldsymbol{M}_{leg_2}\boldsymbol{M}_{free}] &= \boldsymbol{M}_{\dot{\theta}} \\ [\boldsymbol{H}_{leg_1}\boldsymbol{H}_{leg_2}\boldsymbol{H}_{free}] &= \boldsymbol{H}_{\dot{\theta}}. \end{aligned}$$

By substituting Eq.(7), we obtain the momentum equation under the constraint as

$$\begin{bmatrix} \boldsymbol{P} \\ \boldsymbol{L} \end{bmatrix} = \begin{pmatrix} \boldsymbol{M}_{\xi_B} & \boldsymbol{M}_{free} \\ \boldsymbol{H}_{\xi_B} & \boldsymbol{H}_{free} \end{pmatrix}\begin{bmatrix} \boldsymbol{\xi}_B \\ \dot{\boldsymbol{\theta}}_{free} \end{bmatrix} + \sum_{n=1}^{2}\begin{pmatrix} \boldsymbol{M}_{\xi_F i} \\ \boldsymbol{H}_{\xi_F i} \end{pmatrix}\boldsymbol{\xi}_{F_i}, \tag{10}$$

where

$$\boldsymbol{\xi}_B \equiv [\boldsymbol{v}_B^T \quad \boldsymbol{\omega}_B^T]^T$$

$$
\begin{aligned}
\boldsymbol{\xi}_{F_i} &\equiv [\boldsymbol{v}_{F_i}^T \quad \boldsymbol{\omega}_{F_i}^T]^T \\
\begin{pmatrix} \boldsymbol{M}_{\xi_B} \\ \boldsymbol{H}_{\xi_B} \end{pmatrix} &\equiv \begin{pmatrix} \tilde{m}\boldsymbol{E} & -\tilde{m}\widehat{\boldsymbol{r}_{B\to c}} \\ \boldsymbol{0} & \tilde{\boldsymbol{I}} \end{pmatrix} \\
&\quad - \sum_{n=1}^{2} \begin{pmatrix} \boldsymbol{M}_{\xi_F i} \\ \boldsymbol{H}_{\xi_F i} \end{pmatrix} \begin{pmatrix} \boldsymbol{E} & \widehat{\boldsymbol{r}_{B\to F_i}} \\ \boldsymbol{0} & \boldsymbol{E} \end{pmatrix} \\
\begin{pmatrix} \boldsymbol{M}_{\xi_F i} \\ \boldsymbol{H}_{\xi_F i} \end{pmatrix} &\equiv \begin{pmatrix} \boldsymbol{M}_{leg_i} \\ \boldsymbol{H}_{leg_i} \end{pmatrix} \boldsymbol{J}_{leg_i}^{-1}.
\end{aligned}
$$

The second term in the right hand side of Eq.(10) indicates the extra momentum generated by specifying the foot speed.

4 Momentum Control

Following the result of the last section, we propose the Momentum Control, which is a method to generate the whole body motion of a humanoid robot such that the resulted total momentum becomes the spcified value. By this method, we can generate not only a running pattern but also various dynamic motions.

4.1 Setting momentum reference

For every mechanical system, no matter how its structure or behavior is complicated, we can determine the position of the CoM $\tilde{\boldsymbol{c}}$, the linear momentum $\boldsymbol{P}$ and the angular momentum $\boldsymbol{L}$ for the total mechanism.

Dividing the total linear momentum $\boldsymbol{P}$ by the total mass $\tilde{m}$, we obtain the translational speed of the CoM.

$$
\frac{d}{dt}\tilde{\boldsymbol{c}} = \frac{\boldsymbol{P}}{\tilde{m}} \tag{11}
$$

Thus, we can control the position of the CoM by manipulating the translational momentum.

As the extension of this, we propose a method of control or pattern generation by manipulating the total (linear and angular) momentum. Let us call this method the *Momentum Control*. The reference motion of a humanoid robot can be specified assuming a rigid body whose mass and moment of inertia are equal to the target. However, we cannot associate the orientation of this imaginary rigid body to the robot, since a rigid body does not hold enough information to represent the internal structure of the robot system.

4.2 Momentum selection and control by pseudo-inverse

In many applications, we do not have to specify all six elements of the momentum. Moreover, in some case the problem becomes numerically unstable when we specify the all elements of the reference momentum. Therefore, we introduce a selection matrix $\boldsymbol{S}$ which is $n \times 6$ ($0 < n \leq 6$) to pick up the elements of the momentum to be controlled. The selection of the momentum is given by

$$
\boldsymbol{S} \equiv \begin{bmatrix} \boldsymbol{e}_{S_1}^T \\ \vdots \\ \boldsymbol{e}_{S_n}^T \end{bmatrix}, \tag{12}
$$

where $\boldsymbol{e}_i$ is a column vector of 6×1 that has one at i-th element and zeros for the rest. S_i specifies the element of the momentum we want to pick up. Transposing the second term of Eq.(10) from the right side to the left side and multiplying $\boldsymbol{S}$ from left, we obtain the following equation

$$
\boldsymbol{y} = \boldsymbol{A} \begin{bmatrix} \boldsymbol{\xi}_B \\ \dot{\boldsymbol{\theta}}_{free}, \end{bmatrix} \tag{13}
$$

where

$$
\begin{aligned}
\boldsymbol{y} &\equiv \boldsymbol{S}\left\{ \begin{bmatrix} \boldsymbol{P}^{ref} \\ \boldsymbol{L}^{ref} \end{bmatrix} - \sum_{n=1}^{2} \begin{pmatrix} \boldsymbol{M}_{\xi_F i} \\ \boldsymbol{H}_{\xi_F i} \end{pmatrix} \boldsymbol{\xi}_{F_i}^{ref} \right\} \qquad (14) \\
\boldsymbol{A} &\equiv \boldsymbol{S} \begin{pmatrix} \boldsymbol{M}_{\xi_B} & \boldsymbol{M}_{free} \\ \boldsymbol{H}_{\xi_B} & \boldsymbol{H}_{free} \end{pmatrix}. \qquad (15)
\end{aligned}
$$

$\boldsymbol{P}^{ref}$ is the reference linear momentum, $\boldsymbol{L}^{ref}$ is the reference angular momentum and $\boldsymbol{\xi}_{F_i}^{ref}$ is the reference velocity for each foot.

Using Eq.(13), the target speed which realize the reference momentum and the speed $(\boldsymbol{\xi}_B^{ref}, \dot{\boldsymbol{\theta}}^{ref})$ is calculated as the least square solution by

$$
\begin{bmatrix} \boldsymbol{\xi}_B \\ \dot{\boldsymbol{\theta}}_{free} \end{bmatrix} = \boldsymbol{A}^{\dagger}\boldsymbol{y} + (\boldsymbol{E} - \boldsymbol{A}^{\dagger}\boldsymbol{A}) \begin{bmatrix} \boldsymbol{\xi}_B^{ref} \\ \dot{\boldsymbol{\theta}}_{free}^{ref} \end{bmatrix}. \tag{16}
$$

This equation gives the Momentum Control. The proposed method can be regarded as the generalized scheme of conventional control methods for humanoid robot. Sano and Furusho proposed a control of the angular momentum to stabilize their biped robot [14], and the second author proposed a dynamic balancing of humanoid using the angular momentum [8]. Kagami et al. [7] proposed a balance control method of a humanoid by manipulating the CoM with second order nonlinear programming optimization, and Sugihara et al. proposed a balancing and walking controller based on the CoM manipulation [15]. Their methods correspond to a control of the linear momentum. Particularly, their *COG Jacobian* [7, 15] can be obtained when we divide the matrices $\boldsymbol{M}_{\xi_B}$ and $\boldsymbol{M}_{free}$ of Eq.(10) by the total mass $\tilde{m}$.

4.3 Running pattern generation by momentum control

The running pattern is planned using a simple inverted pendulum, and then transformed into the

command for a humanoid model. In our previous report[9], to generate the running pattern, we applied the CoM of the inverted pendulum to Σ_B and the contact point of the inverted pendulum to Σ_{F_1} or Σ_{F_2}(Figure 2). With this method, a robot could not correctly perform the planned motion, and we had to modify the pattern. By using the momentum control and applying the pattern based on an inverted pendulum to the linear momentum $\boldsymbol{P}^{ref}$, the correct hopping and running patterns can be generated.

Furthermore, in previous report, we introduced arm swing in ad hoc manner to compensate the *yaw* moment genarated by the swing leg. The same compensation can be realized by the Momentum Control with given reference of the angular momentum $\boldsymbol{L}^{ref}$ whose *yaw*-axis elment is set to be zero. Although HRP-2L does not have arms, the *yaw* moment is suppressed by the body rotation, which is automatically generated by the Momentum Control.

5 Optimal Hopping Pattern

Unlike Raibert's hopping robots which utilize natural oscillation of spring-mass system[13], our robot allows precise control of hopping support phase. Therefore, we can seek an optimal vertical hopping pattern which minimizes required power. We use a simple model as Figure 3, and assume steady hopping with the support period of T_s and the flight period of T_f. From preliminary simulation, we decided those period as $T_s = 0.18[s]$ and $T_f = 0.08[s]$ which mostly gives realizable running motions.

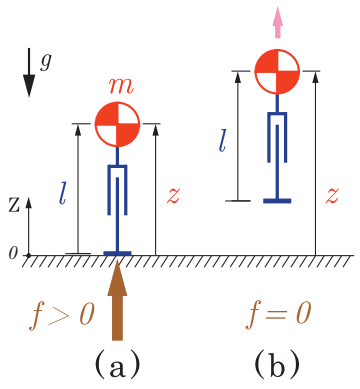

Figure 3: *Inverted pendulum model for examination*

While the foot is in contact with the ground(Fig.3(a)), the motion equation of CoM is given by

$$\ddot{z} = -g + \frac{f}{m}, \tag{17}$$

where z is the height of CoM, f is the vertical force, m is the mass of the robot, g is gravity acceleration. While the robot is flying(Fig.3(b)), as CoM moves parabolic, there is a relationship as follows,

$$\begin{cases} \dot{z}_t - \dot{z}_l = gT_f \\ z_t - z_l = \frac{1}{2}gT_f{}^2 \end{cases} \tag{18}$$

where z_t and $\dot{z}_t$ are the height and the velocity at takeoff, z_l and $\dot{z}_l$ are the height and the velocity at landing.

To minimize the required power for hopping, we specify the performance index as

$$J_{index} = \int_0^{T_s} (\dot{z}f)^2 dt. \tag{19}$$

The hopping pattern that minimizes J_{index} subject to Eq.(17) with terminal condition of Eq.(18) is calculated by numerical method. The obtained pattern is shown in Figure 4.

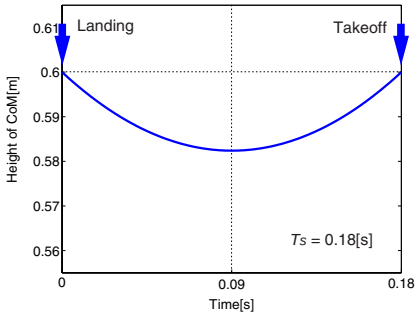

Figure 4: *Optimal hopping trajectory*

6 Simulation

For the dynamic simulation, we use OpenHRP simulator which was also developed in the Humanoid Robotics Project(HRP)[3]. The robot data is given by an extended VRML format which combines dynamic parameters and the geometric shape of the links. The effect of the rotor inertia of the servomotors can be also considered. In the simulation, the joint angles and the angular velocities are calculated by the Momentum Control and served as the reference for the PD feedback control.

At first, we check the possibility of the countinuous vertical hopping of HRP-2L. The vertical linear momentum of the hopping in the last section is applied as the reference. In addition, we apply a constant pitch inclination of $\pi/6$ radian to the body, because it reduces the load of the knee joints effectively.

In this vertical hopping simulation, the CoM of HRP-2L goes up and down for 2.5[cm]. For this motion, it is considered that the hip pitch joints, the

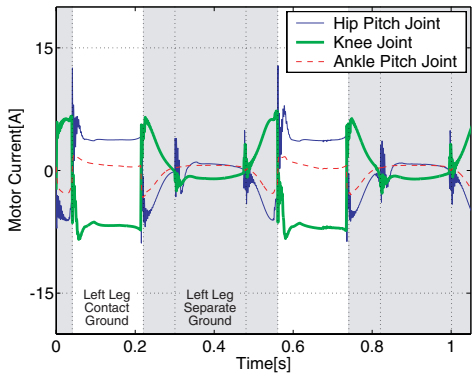

Figure 5: *Motor current for hopping*

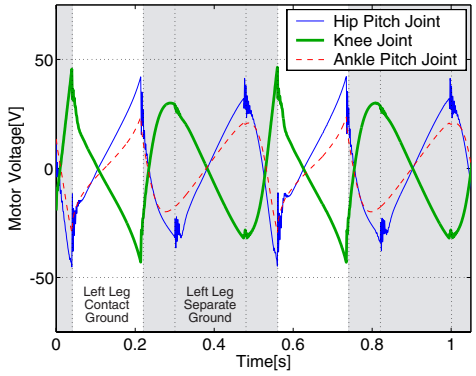

Figure 6: *Motor voltage for hopping*

knee joints and the ankle pitch joints take most important role. Figures 5 and 6 show motor current and motor voltage of those joints of left leg, respectively. In each graph, the horizontal dotted lines indicate permitted value and the vertical dotted lines indicate the timing of phase transition. All of the actuators operate within their permitted values. Figure 7 shows those rotor temperature. The horizontal dotted line indicates rotor's permitted temperature. Although rotors of the hip and knee joint motor finally reach the permitted temperature, the robot can perform hopping longer than 30[s] until that time.

In the same way, we also confirmed that HRP-2L can run with 0.5[m/s](Figure 8). Values of motor current and voltage are within theirs permitted values, and Figure 9 shows that all of motors can work 40[s] at least, and the robot can travel 20[m].

To realize a running humanoid, the impact magnitude at landing is an important term. Figure 10

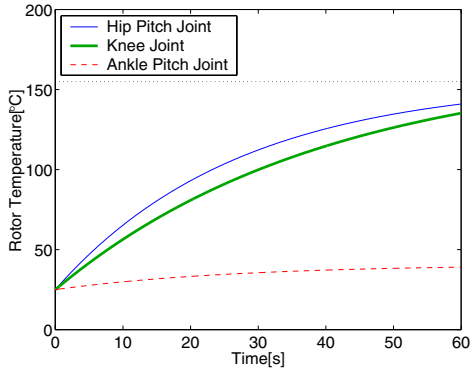

Figure 7: *Rotor temperature for hopping*

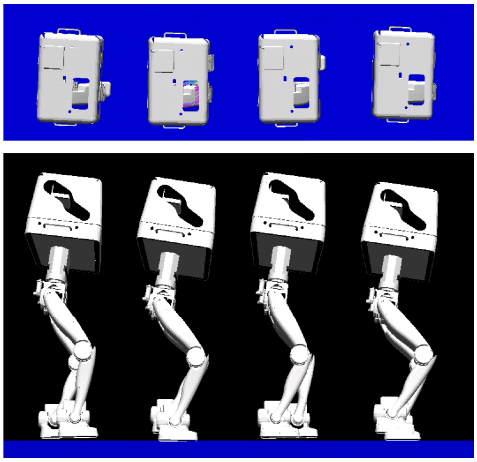

Figure 8: *Running robot at 2.8 2.9 3.1 3.2 [s] (top: top view, bottom: side view)*

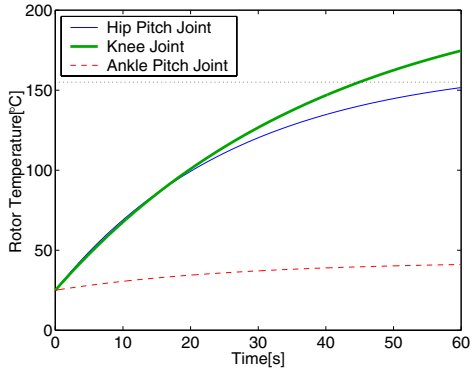

Figure 9: *Rotor temperature for running at 0.5[m/s]*

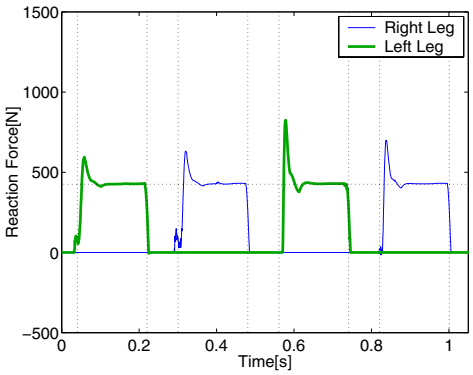

Figure 10: *Reaction force for running at 0.5[m/s]*

shows the vertical reaction force of each legs corresponding the running of Figure 8. In this graph, the horizontal dotted line indicates the force expected from the inverted pendulum model. The peak of the reaction force is 840[N]. This is only about 1.5 times of weight of the original HRP-2L with dummy weight and the impact of similar magnitude was frequently measured in its walking experiments. Therefore, we can conclude that our robot has enuogh strength to perform the proposed running motion. By using the Momentum Control, the motion of multi-link model as a humanoid robot corresponds to the planned motion based on a simple inverted pendulum well.

7 Conclusions

In this paper, we presented a possibility of running humanoid robot based on the physical properties of an existing humanoid robot HRP-2L. To generate running motion, we developed a general method to control the total linear/angular momentum of multi-link system. We named the method the Momentum Control. By this method, we could generate a reliable running pattern. Conducting simulations which took into account of physical restrictions, we showed that our humanoid robot can run at least with 0.5[m/s]. The running experiment with HRP-2L hardware is our next target.

References

[1] Ahmadi,M. and Buehler,M., "The ARL Monopod II Running Robot: Control and Energetics", Proc. of the 1999 ICRA, pp.1689-1694, 1999.

[2] Gienger, M., et.al, "Toward the Design of a Biped Joggind Robot," Proc. of the 2001 ICRA, pp.4140-4145, 2001.

[3] Hirukawa, H., Kanehiro, F., Kajita, S., "OpenHRP: Open Architecture Humanoid Robotics Platform," Intr. Symposium on Robotics Research (ISRR), Melbourne, 2001

[4] Hirai, K., Hirose,M., Haikawa, Y. and Takenaka, T., "The Development of Honda Humanoid Robot," Proc. of the 1998 ICRA, pp.1321-1326, 1998.

[5] Hodgins, J. K.,"Three-Dimensional Human Running," Proc. of the 1996 ICRA, pp.3271-3277, 1996.

[6] Inoue, H., Tachi, S., Nakamura, Y., Hirai, K., et.al, "Overview of Humanoid Robotics Project of METI," Proc. Int. Symp. Robotics, pp.1478-1482, 2001.

[7] Kagami, S., Kanehiro, F., Tamiya, Y., Inaba, M., and Inoue, H., "AutoBalancer: An Online Dynamic Balance Compensation Scheme for Humanoid Robots," Proc. of the 4th Inter. Workshop on Algorithmic Foundation on Robotics (WAFR'00), 2000.

[8] Kajita, Yokoi, Saigo and Tanie: Balancing a Humanoid Robot Using Backdrive Concerned Torque Control and Direct Angular Momentum Feedback, Proc. of ICRA2001, pp.3376-3382 (2001).

[9] Kajita. S. et. al.,"Running Pattern Generation for a Humanoid Robot", Proc. of the 2002 ICRA, pp.2755-2761, 2002.

[10] Kenji, K. et. al.,"Design of Advanced Leg Module for Humanoid Robotics Project of METI", Proc. of the 2002 ICRA, pp.38-45, 2002.

[11] Nishiwaki, K., Sugihara, T., Kagami, S., Kanehiro, F., Inaba, M., and Inoue, H., "Design and Development of Research Platform for Perception-Action Integration in Humanoid Robot: H6," Proc. Int. Conference on Intelligent Robots and Systems, pp.1559-1564, 2000.

[12] Playter, Robert R. and Raibert, Marc H., "Control of a Biped Somersault in 3D," Proc. of IFToMM-jc International Symposium on Theory of Machines and Mechanisms (in Nagoya, Japan), pp.669-674, 1992.

[13] Raibert, M., *Legged Robots that Balance*, Cambridge, MA, MIT Press, 1986.

[14] Sano, A. and Furusho, J. , "Realization of Natural Dynamic Walking Using The Angular Momentum Information," Proc. of ICRA1990, Cincinnati, 3, pp.1476-1481, 1990.

[15] Sugihara, Nakamura and Inoue: Realtime Humanoid Motion Generation through ZMP Manipulation based on Inverted Pendulum Control, Proc. of ICRA 2002, pp.1404-1409 (2002).

[16] Yamaguchi, J.,Soga,E., Inoue, S. and Takanishi, A., "Development of a Bipedal Humanoid Robot – Control Method of Whole Body Cooperative Dynamic Biped Walking –," Proc. of the 1999 ICRA, pp.368-374, 1999.